Competing Modes in Erbium Doped Fiber Ring Lasers

M. Kamil Abd-Rahman[1], S. Selvakennedy[2] and Harith Ahmad[2]

[1] Faculty of Applied Science, Universiti Teknologi Mara,
40450 Shah Alam, Selangor, Malaysia
Tel: 60-3-5544 4602, Fax: 60-3-5544 4562
e-mail: mohdkamil.abdrahman@physics.org
[2] Department of Physics, Faculty of Science, University of Malaya
50603 Kuala Lumpur, Malaysia
e-mail: harith@umcsd.um.edu.my

Abstract: The erbium doped fibre ring laser (EDFL) is modelled using the standard propagation and rate equations of a homogeneous, two-level gain medium. The EDFL numerical simulations provide comparable results with the experimental data. The process of lasing mode competition and mode selection is clearly depicted and explained.

1. Introduction

The EDFL have gained tremendous interest for applications in optical telecommunication systems as the potential compatible laser sources [1,2] with high output powers and narrow linewidths. Much work has been investigated [3,4] into the behaviour of erbium-doped fiber ring lasers (EDFL). However, the modelling activities of the EDFL is not as extensive as compared to the erbium-doped fiber amplifier (EDFA) system.

Here we present a rigorous numerical model for the analysis of a continuous wave operation of an EDFL. The simulation is developed as an enhancement to the EDFA model by incorporating the feedback mechanism for the cyclical propagation in the cavity [5]. The results of the laser model in a steady state condition are values that are cross-checked with the experiment data.

Using the numerical approach for the model allows the study of the ring laser behaviour during its transient period, which is not readily investigated using the experimental approach. The manner in which the modes compete before lasing in the ring cavity and the process of lasing mode selection are well depicted in the model. The numerical simulation could provide useful comparable results for the EDFL lasing wavelength.

2. Theory And Model

The model assumes that the pump level 3 of the 3-level system remains nearly empty because of the rapid transfer of the pump population to the excited state 2, hence a 2-level system is considered. Pumping into the 980nm-absorption band implies that the population in the $^4I_{11/2}$ manifold is negligible. This assumption is valid for EDF systems whereby the ion lifetime at the pumping level is very much smaller than that at the metastable level [6].

The EDFL is described in a cylindrical co-ordinate system (r, ϕ, z) with z as the fibre axis. The numerical simulation of the EDFL based on the two-level homogeneous medium transition is described by the standard population rate equations [5]:

$$N_2(r,z) = \sigma_{Er}(r)\frac{R_{pa}(r,z)+W_{sa}(r,z)}{R_{pa}(r,z)+W_{se}(r,z)+W_{sa}(r,z)+A_e} \quad (1)$$

$$N_1(r,z) = \sigma_{Er}(r) - N_2(r,z) \quad (2)$$

where N_1 and N_2 are ions concentrations at level 1 and 2, R_{pa} is the pump absorption rate, W_{sa} and W_{se} are signal absorption and emission rates, respectively and A_e is the spontaneous emission rate.

In this simulation, the approach taken in describing the evolution of the propagating energy of the pump and signal is by the segmentation of the wavelength spectrum into many slots. The pump power P_p, signal power P_s, and ASE$^{\pm}$ power are then analyzed by use of the standard propagation equations within each individual slot.

$$\frac{dP_p(z)}{dz} = -\gamma_a(\nu_p,z)P_p(z) \quad (3)$$

$$\frac{dP_S(z)}{dz} = [\gamma_e(\nu_S,z)-\gamma_a(\nu_S,z)]P_S(z) \quad (4)$$

$$\frac{dS^{\pm}_{ASE}(\nu,z)}{dz} = \{\pm 2h\nu\gamma_e(\nu,z) \pm [\gamma_e(\nu,z)-\gamma_a(\nu,z)]\cdot S^{\pm}_{ASE}(\nu,z)\} \quad (5)$$

where h, $\gamma_e(\nu,z)$ and $\gamma_a(\nu,z)$ is Planck's constant, emission and absorption factors at frequency ν, determined from the emission and absorption cross-section respectively and the overlap integral between the mode and the population concentration in the excited and the ground state.

The signal, and forward/backward ASE (ASE$^{\pm}$) are presented in 580 wavelength slots from λ = 1420nm to 1620nm. In each step, the overlap integrals involved are solved numerically in 40 equal interval points from $r = 0$ to $r = a$, where a is the core radius of the fiber. Equations (3)-(5) are a set of coupled differential equations that can be solved numerically by means of an iterative procedure, whose convergence speed is influenced by the width and the number of slots used.

3. Numerical Results

The spectral model requires input data that can be obtained through experimental measurements on the active fiber. The absorption and emission cross-section of the erbium doped fiber, together with the fiber parameters, the pump powers and the ratio of the linear ion density to the metastable lifetime, represent the input data for the numerical simulations. The modeled fiber has core radius of 1.68μm, fiber length of 7.0m and a step-index profile with a numerical aperture (NA) of 0.22, and an assumed uniform doping of erbium ion concentration of 240ppm. The total cavity loss of the EDFL was about 2.3dB, inclusive of component insertion losses and splice losses but excluding the output coupling loss.

The schematic of the fiber ring laser considered for the numerical simulations and used for experimental verification is depicted in Figure 1. The resonator was pumped with a 980nm-laser diode via a WDM coupler launching a continuous power necessary to provide population inversion into the doped fiber. The optical isolator ensures unidirectional operation of the laser while the output coupler outputs the laser signal for monitoring.

To model the ring laser, the output signals of the doped fiber amplifier are carried back to the input, which provides the feedback mechanism for the laser. The ASE^{+} generated during the first run becomes the input signal of the second run. Only the ASE^{+} is being considered and allowed to propagate since the optical isolator restrain the propagation of ASE^{-}. During each run, the signal is amplified based on the amplifier model using the relaxation approach. The output is then compared for the threshold condition before being fed back for the next run. Only the wavelengths whose gains fulfil the threshold condition are allowed for further feedback, hence the oscillation.

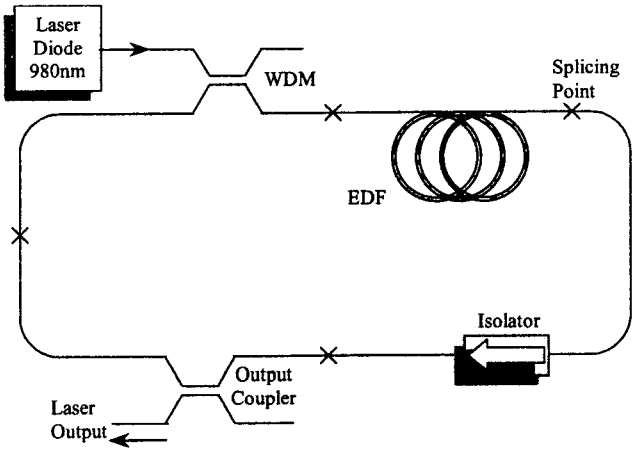

Figure 1: Schematic of the Er^{3+} doped fiber ring laser.

At the output of each loop, the wavelength spectrum is compared, slot by slot, with the input; the highest relative difference is considered as the current convergence error. The procedure stops as soon as this error drops below a given tolerance, which is taken here as 10^{-4}. The behaviour of the ring laser is strongly determined by the open-chain behaviour of the amplifier, whose saturation conditions are essential to describe the lasing effect [7].

Figure 2 illustrates the gain evolution of three competing modes in the ring cavity. The simulated result was taken for up to 70 oscillations from the EDFL with configuration comprising of a 7.0m long EDF, a 3dB output coupler (represents 50% reflectivity) and the laser was pumped with 50mW of power. The system was first started off as an amplifier whereby the ring cavity was opened. The first oscillation started from the moment the opened cavity was looped to form a closed ring. The 3dB directional coupler was used to provide the oscillation feedback.

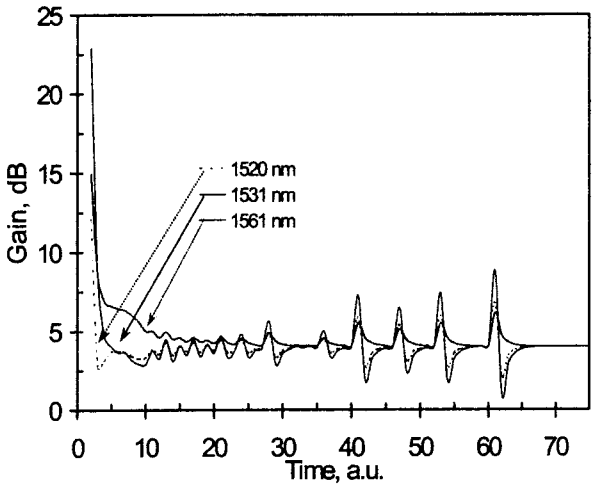

Figure 2: The gain evolutions in the ring cavity before steady-state.

The gain starts at very high values for the three modes i.e. 12.5dB at 1520nm, 23dB at 1531nm and 15dB at 1561nm, where the mode at 1531nm experiences the highest level due to its highest emission factor. However, its gain drops very fast due to saturation and the moment the feedback mechanism is provided. When 1531nm saturates, it also saturates the gain for the other signals due to the transient cross-gain saturation effect, and causes their gain to be greatly reduced [8].

This is a standard case for an EDFA with sufficient pump power in which the gain is the highest at 1530nm, followed by that at 1560nm. This is especially true at wavelengths of 1520nm and 1531.02nm, which show a very sharp downfall. The gain at 1561.02nm shows a rather transient decrement. The slower decrement of the gain at the longer wavelength is consistent with the result obtained by Desurvier [9].

When the mode at the 1531nm dies off, the gain of 1561nm stops falling drastically and it builds up power as shown in Figure 3. It is notable that in Figure 2 there are a number of ringing occurring during the course of oscillation and these ringing become even more obvious as the system closes to its steady state. Ringing occurs whenever a particular mode dies when competing between one another. The higher the strength of the dying modes, the more significant the ringing becomes. Thus, at initially stage where the powers of the modes were smaller, the ringing was smaller. As more modes die out, the number of

remaining modes is reduced with consequently gaining higher strengths and the ringing becomes even stronger.

In Figure 3, the steps seen in the 1561nm-power evolution is due to the dying modes, observed from the ringing. Whenever a ringing occurs, the absolute power of the remaining modes grows a step higher by extracting power from the dying modes. When Figs. 2 and 3 are compared, it is observed that beyond 40 units of time, there are four occurrences of ringing corresponding to the four steps in the signal power evolution. When the mode selection is over, the system settles down in terms of both gain and signal power. In this laser configuration, it lased at 1561nm. In Figure 2, it is also seen that the gain settles down around a common line, which is almost equivalent to the cavity loss.

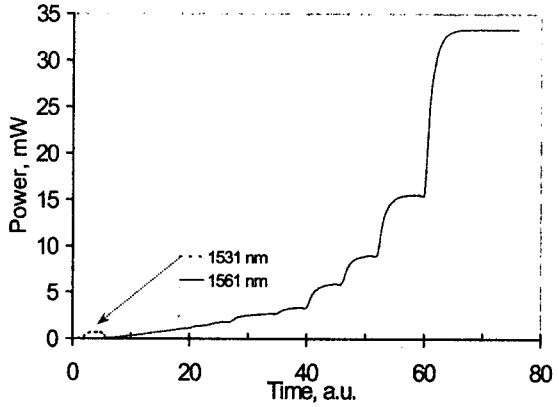

Figure 3: The calculated absolute signal power evolutions in the ring cavity before steady-state.

Figure 4 shows the formation of output spectra during its transient state for various time intervals. During the initial stage of the transition, higher number of modes is sustained by the cavity as shown by the broader output spectra. However, as some modes saturates and consequently lose power to other modes, the spectral width becomes narrower, thus the powers of the competing modes are higher. This phenomenon is consistent with the earlier results and the observed stronger ringing as the system settles down. After 70 units of the arbitrary time, the system settles down and lases at 1561nm. These results clearly demonstrate the process of mode selection that occurs in the cavity.

The numerical results are compared to the experimental data obtained during the steady state for verification of the model. The numerical plot of the EDFL emission wavelength versus the output coupler reflectivity shows comparable results with the experimental data as shown in Figure 5. The plots show good match between the two approaches, hence verifying the accuracy of the adopted numerical model. For lower reflectivity, the EDFL tends to lase at shorter wavelength, while at higher reflectivity, the system shifts to longer wavelength at around 1560nm. The output coupler reflectivity resolves the output power from the laser and the amount of light that is allowed to oscillate in the ring. A cavity with low reflectivity permits a relatively a small amount of signal to propagate in the ring and outputs a relatively high power. This is because the energy available for oscillation is limited and the mode with the highest absorption coefficient tends to accumulate the energy and this mode is likely to lase. However, when the coupling into the cavity is high, the shorter wavelengths tend to saturate its gain. This enables the modes at longer wavelengths to accumulate energy and are more likely to lase.

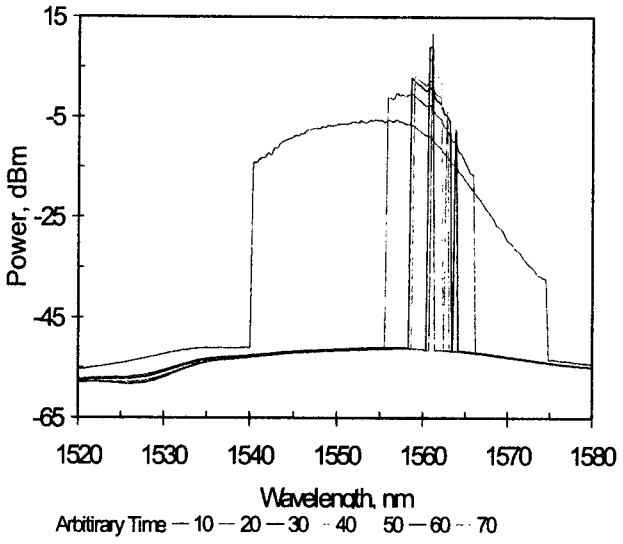

Figure 4: The calculated output spectrum of the ring cavity before steady-state for arbitrary time interval.

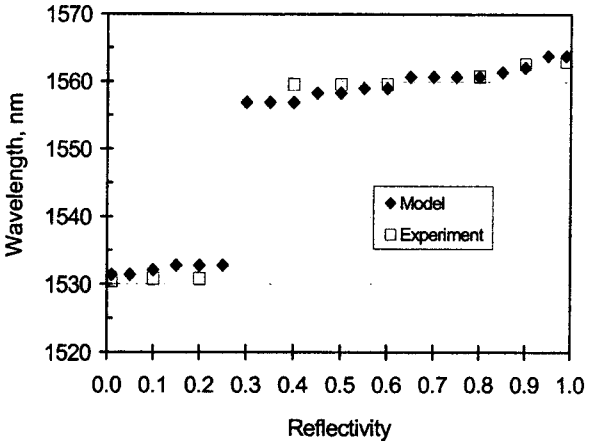

Figure 5: EDFL operating wavelength as a function of output coupler reflectivity.

4. Conclusions

In this paper, the numerical method for modelling the laser oscillation has been described using the homogeneous two level approximation of amplification in erbium doped fibres. Comparable numerical results with the experimental measurements have been achieved with more than 90% accuracy. The model clearly depicted the lasing mode selection process in the ring cavity during the transient

period. The model can also provide information about the peak power of the lasing signal and lasing characteristics. No polarization sensitive devices have been considered in the model, as it cannot provide a vectorial analysis. And also, no nonhomogeneous line broadening effects have been considered, thus this model could not provide information about the linewidth of the laser. The numerical model can accommodate for a mode-selective element (optical filter) in the ring cavity by restricting feedbacks from other modes such that only modes within the filter bandwidth are allowed to oscillate.

5. References

[1] C. V. Poulsen and M. Sejka, "Highly optimized tunable Er^{3+}-doped single longitudinal mode fiber ring laser, experiment and model", *IEEE Photon. Technol. Lett.*, vol. 5, no. 6, pp. 646-648, 1993.

[2] P. L. Scrivener, E. J. Tarbox, and P. D. Maton, "Narrow linewidth tunable operation of erbium doped single mode fiber laser", *Electron. Lett.*, pp. 549-551 1989.

[3] M. Mignon and E. Desurvire, "An analytical model for the determination of optimal output reflectivity and fiber length in erbium-doped fiber lasers", *IEEE Photon. Technol. Lett.*, vol. 4, no. 8, pp. 850-852, 1992.

[4] K. Iwatsuki, H. Okamura, and M. Saruwatari, "Wavelength-tunable single-frequency and single-polarization Er-doped fiber ring laser with 1.4kHz linewidth", *Electron. Lett.*, vol. 26, pp. 2033-2035, Nov 1990.

[5] B. Pedersen, A. Bjarklev, J. H. Povlsen, K. Dybdal and C. C. Larsen, "The design of erbium-doped fiber amplifiers," *J. of Lightwave Technology*, Vol. 9 No. 9, (1991), 1105-1112.

[6] R. J. Mears, "Optical fiber Lasers and Amplifiers," *PhD Thesis*, University of Southampton, UK, 1998.

[7] S. Cucinotta, S. Dallargine, Selleri, C. Zilioli, and M. Zoboli, "Modeling of erbium doped fiber ring laser," *Optics Communications*, Vol. 141, (1997), 21-24.

[8] S. R. Chinn, "Simplified modeling of transients in gain-clamped erbium-doped fiber amplifiers," *J. of Lightwave Technology*, Vol. 16 No. 6, (1998), 1095-1100.

[9] E. Desurvire, "Principles and Applications of Erbium Doped Amplifiers," *John Wiley and Sons*, 1994.